Design, fabrication, and testing of lumped element kinetic inductance detectors for 3 mm CMB Observations

Amy E. Lowitz[a], Ari-David Brown[b], Thomas R. Stevenson[b], Peter T. Timbie[a] and Edward J. Wollack[b]

[a]University of Wisconsin - Madison, Madison, WI, USA;
[b]NASA Goddard Space Flight Center, Greenbelt, MD, USA

ABSTRACT

Kinetic inductance detectors (KIDs) are a promising technology for low-noise, highly-multiplexible mm- and submm-wave detection. KIDs have a number of advantages over other detector technologies, which make them an appealing option in the cosmic microwave background B-mode anisotropy search, including passive frequency domain multiplexing and relatively simple fabrication, but have suffered from challenges associated with noise control. Here we describe design and fabrication of a 20-pixel prototype array of lumped element molybdenum KIDs. We show Q, frequency and temperature measurements from the array under dark conditions. We also present evidence for a double superconducting gap in molybdenum.

Keywords: kinetic inductance detectors, cosmic microwave background, CMB, KID, Molybdenum

1. INTRODUCTION

Kinetic inductance detectors (KIDs)[1] are a type of pair-breaking, superconducting, incoherent detector for millimeter and sub-millimeter radiation. They have undergone rapid development in the last decade. KIDs have a broad range of applications in astronomy, quantum computation, parametric amplifiers, and other efforts.[3] However as a result of the fundamental requirement that the incident radiation be pair-breaking and of practical limitations on base temperature, for lower-energy incident radiation it is more difficult to design a practical KID that will not be limited by thermal noise at practical bath temperatures. One of the primary aims of this work is to push the long wavelength limit of KIDs in order to make them useful for cosmic microwave background (CMB) applications. The detectors described in this work were designed for the 100 GHz module of the QUBIC telescope,[2] a bolometric interferometer which will be fielded at the Concordia Station in Antarctica for studying CMB polarization.

2. DESIGN

We selected Mo for the resonator layer due to constraints on T_c, the superconductor critical temperature; we require a $T_c \lesssim 1.3$ K to be pair-breaking with 100 GHz radiation, and $T_c \gtrsim 0.7$ K to avoid being thermal noise dominated at our laboratory base temperature of 150 mK. $T_c = 0.915$ for bulk samples of Mo and is higher for very thin films. TiN is another material that can meet these T_c requirements and has other desirable properties for KIDs, including quasiparticle recombination time and density of states. However due to fabrication challenges we decided to work with Mo at present; we plan to pursue TiN in future rounds of fabrication. In order to achieve the high sheet resistance required to attain a good match to free space and good optical coupling, we require very thin films of Mo. The prototype chip described here has a Mo resonator film with a profilometer-measured thickness of 9 nm. The film is highly tensile (∼900 MPa), however measured sheet resistance and Tc were within the expected range, suggesting that the film is of acceptable quality.

The detector is a lumped-element KID (LEKID) featuring an integrated Nb groundplane (Figure 1, left), on the back side of the wafer, which serves several purposes: it acts as a groundplane for the microstrip resonator and readout transmission line features on the wafer frontside; it provides lossless isolation of the chip

Further author information: (Send correspondence to Amy Lowitz)
Amy Lowitz: E-mail: lowitz@wisc.edu

Millimeter, Submillimeter, and Far-Infrared Detectors and Instrumentation for Astronomy VII, edited by Wayne S. Holland, Jonas Zmuidzinas, Proc. of SPIE Vol. 9153, 91532R · © 2014 SPIE · CCC code: 0277-786X/14/$18 · doi: 10.1117/12.2057102

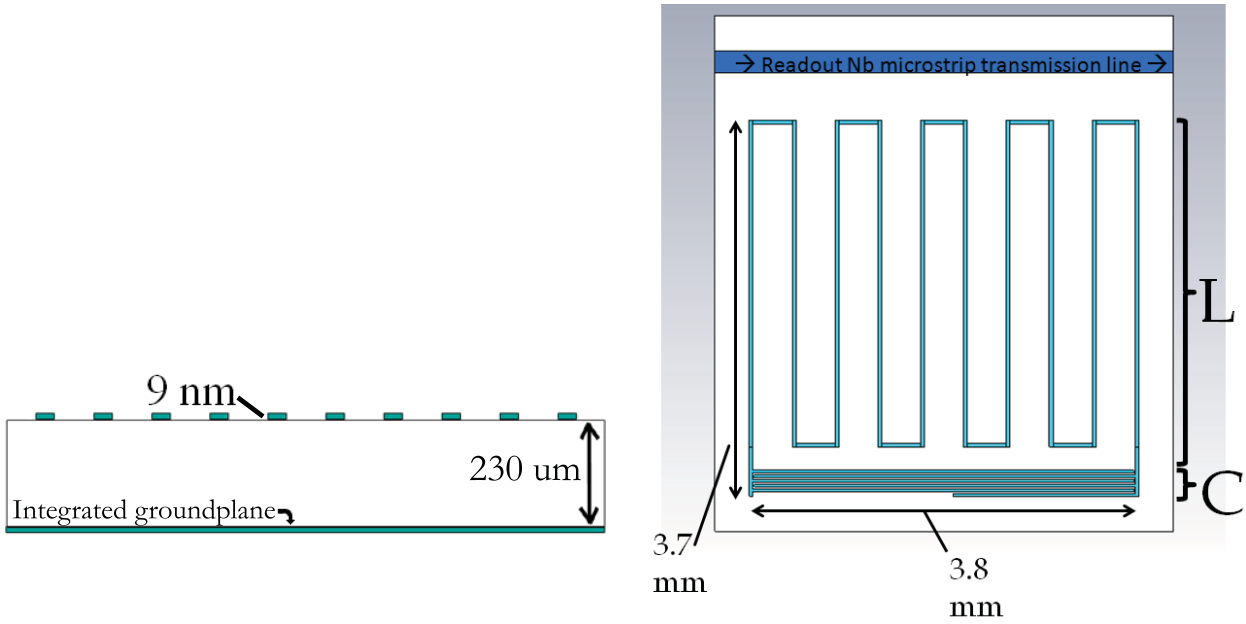

Figure 1. **Left:** Crossection of the inductor section of one pixel, showing the Mo meanders at the top, Si substrate, and the integrated Nb groundplane at the bottom. Not to scale. **Right:** Top view of a single pixel. Note the intermediate length of the 6th interdigitated capacitor finger, which tunes the resonant frequency.

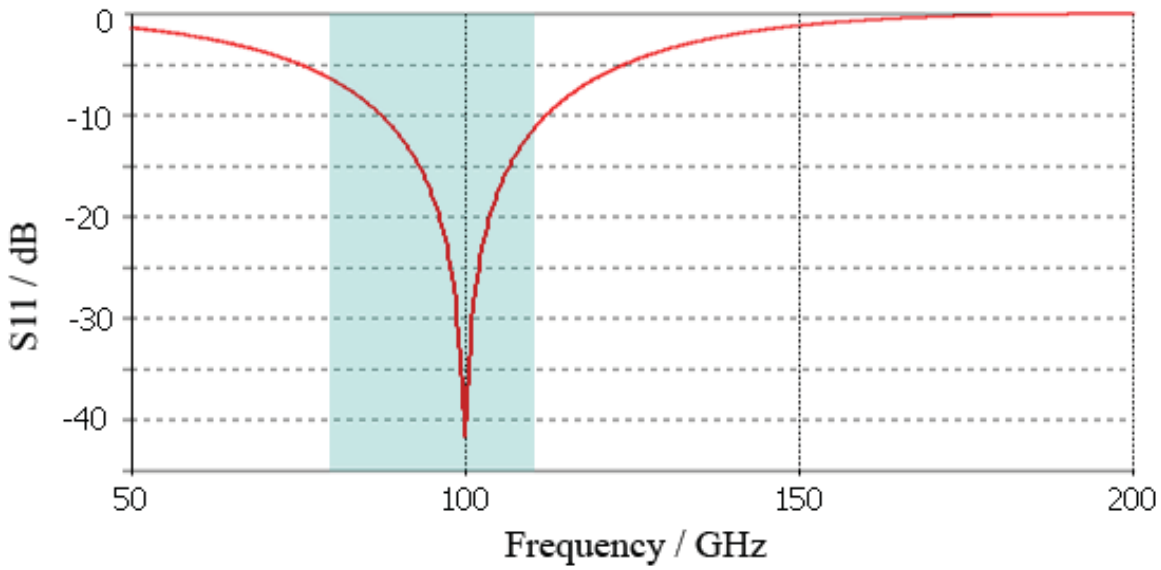

Figure 2. CST simulation of the reflectance of the inductor section of the pixel design. Low reflectance corresponds to high optical efficiency. The highlighted band indicates the frequency range of the ∼100 GHz atmospheric window.

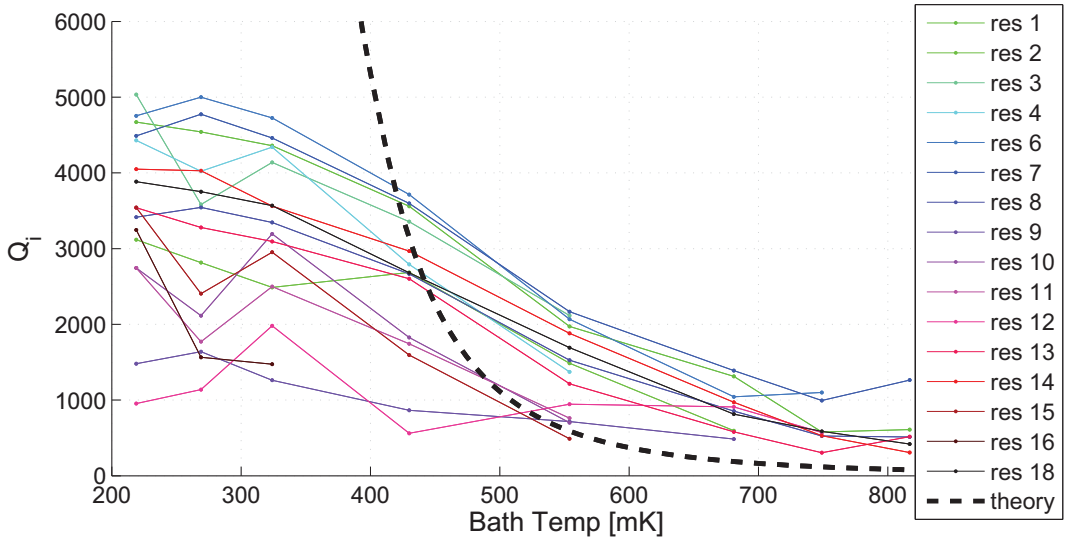

Figure 3. Internal quality factor for the 16 resonators with measurable Qs (resonators 5 and 17 were too faint to measure Q and no data was taken at the 8th resonator's frequency for logistical reasons) are shown over a range of bath temperatures. The heavy dotted black line indicates the theoretical internal Q based on fundamental thermal quasiparticle loading only.

from the lossy copper chip holder package; and it provides a quarterwave backshort for the incoming optical radiation, which substantially improves optical efficiency(Figure 2). To achieve quarterwave spacing for the backshort/groundplane, Si wafers with a made-to-order thickness of 230 $\pm$ 25 μm were specified. The actual thickness of the wafers used was 232 $\pm$ 3 μm. The resonator design (Figure 1) features an inductor with 10 meanders, 33 μm wide, with a pitch of 415 μm. The interdigitated capacitor has 6 fingers with width 20 μm and spacing 20 μm. This results in a geometric inductance of 60 nH, and a capacitance of 1.0 pF. For the the 9 nm thick Mo used for the resonators described here, we expect a kinetic inductance of 31 nH. Therefore, the expected resonant frequency is 527 MHz. The resonant frequencies of the pixels are tuned for multiplexing by varying the length of the last capacitor finger and by adding additional inductor meanders. We have chosen a relatively low readout frequency because of the advantages in reducing TLS noise[3] and because this reduces the cost of some of the room temperature readout electronics.

3. FABRICATION

The prototype detector chips were fabricated in the Detector Development Laboratory at NASA Goddard Space Flight Center. There are three patterned frontside layers plus one unpatterned integrated Nb groundplane/backshort on 40 Ωcm, 230 μm thick Si(001) wafers. At cryogenic temperatures the conductivity of silicon arising from free carriers freezes out and the microwave attenuation is limited by dielectric loss. Frontside layers are: A Nb microstrip readout line, Au heat sinking pads with Ti underlayer for improved adhesion, and Mo microstrip resonators.

4. MEASUREMENTS

Measurements were conducted in a laboratory cryostat, using an adiabatic demagnetization refrigerator (ADR) pre-cooled with a pumped liquid helium bath. Typical base temperatures are $\sim$150 mK, and the temperature of the cold plate can be controlled between the base temperature and $\sim$3 K by ramping the ADR magnet. The ADR is controlled by a 3 T superconducting solenoid magnet which is installed in a magnetically shielded housing to reduce the risk of the ADR field affecting device measurements. Measurements so far have focused on the resonator quality factors and center frequencies under various bath temperature and magnetic field conditions. Future work will seek to measure noise and optical responsivity.

4.1 Resonator Quality Factors

Internal, coupling and total resonator quality factors - Q_i, Q_c, and Q_t respectively - were measured for the 18 detectable resonances on the test chip. At the coldest bath temperatures, the highest Q_is were nearly an order of magnitude lower than expected. The internal Q saturates at a maximum value at low temperature, indicating that there is some unknown source of temperature-independent dissipation which dominates at low temperature. Figure 3 shows the dependence of internal Q on temperature, with 0 normal component of Earth's magnetic field (a discussion of chip orientation with respect to Earth's magnetic field can be found in section 4.2).

4.2 Magnetic Field Trapping

One possible source of Q degradation is magnetic field trapping. If there is a finite magnetic field component normal to the plane of the inductor at the moment when it passes through the superconducting transition, magnetic flux can be trapped by the superconducting material, which can decrease the gap parameter, decreasing Q.[1] In an effort to identify the cause of the degraded internal quality factors, Qs were measured with the cryostat in three different orientations relative to Earth's magnetic field: 180 mG component of B_{Earth} normal to the chip, 47 mG normal to the chip, and 0 mG normal to the chip. The chip was heated above the transition temperature of the Nb groundplane and re-oriented between measurements to ensure all trapped flux during the measurements was associated with the intended cryostat orientation. Error in cryostat orientation is approximately 5°, or about 16 mG.

Results are summarized in Table 1 where a representative sample of measured Q_is for the first 7 detectable resonances are shown at similar temperatures for the three orientations with respect to Earth's magnetic field. As expected, the highest Q_is were observed in the 0 mG normal field orientation, with an average Q_i of 4300 for the 7 resonators shown in detail in the table, or 3500 for all 18 resonators detectable at that temperature. The average Q_i in the maximum normal field component orientation was cut by more than half compared to 0 normal field. The intermediate orientation, at 47 mG, was degraded by about 10% compared to the 0 mG case.

Table 1. Measured Qs for the first 7 detectable resonances. A 180 mG decrease in the normal component of B_{Earth} doubles the average measured Q_i.

Resonance number	**180 mG normal B field, 201 mK**	**0 mG normal B field, 219 mK**	**47 mG normal B field, 204 mK**
1	2100	4700	4900
2	2000	3100	3200
3	2700	5000	3900
4	2200	4400	4100
6	2100	4700	3700
7	2000	4500	3500
9	1500	3400	3700
average Q_i	*2100*	*4300*	*3800*
percent of max	*48%*	*100%*	*89%*

We conclude that magnetic flux trapping can have a significant effect on observed internal resonator quality factors in KID devices, however cryostat orientation is not sufficient to relieve the tension between our measured and expected Qs. Magnetic field orientation will nonetheless be important consideration in the design of KID-based systems requiring high quality factors.

4.3 Double-gap behavior in Mo

A number of superconducting materials are know to exhibit "double-gap" behavior;[4–8] magnesium diboride is especially well-represented in the literature. In a double-gap superconductor, some of the conduction electrons live

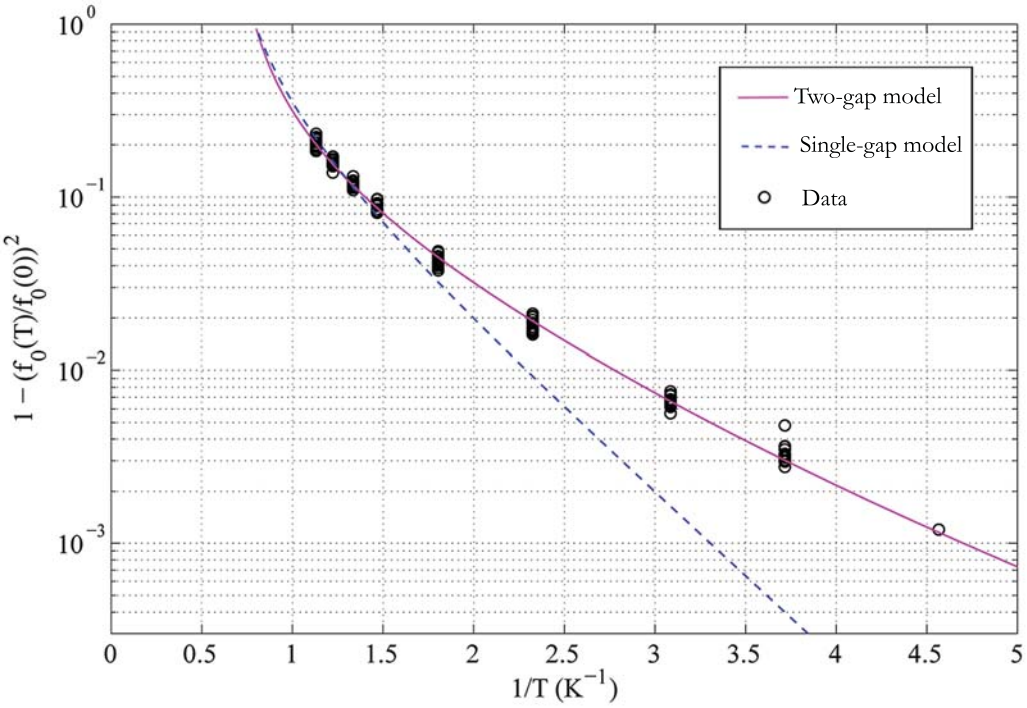

Figure 4. Shown here is the frequency and temperature data (circles), plotted as described in section 4.3. The dashed line is a simple single-gap expectation from Matis-Bardeen with $\alpha = 0.27$ and $\rho = 200\mu\Omega cm$. The solid line is a fit allowing for two superconducting gap energies. Gaps of $0.75 \times \Delta_{BCS}$ and $0.40 \times \Delta_{BCS}$, with 89.9% and 11.1% of the electron states respectively, give the best fit.

in a low-gap state and some live in a high-gap state. Because electrons occupying these states are intermingled in physical space, they proximitize and a simple DC critical temperature measurement reveals a single T_c. However, one expects the internal quality factor in a double gap material to be degraded relative to the Q_i expected based on the DC critical temperature; electrons in the low-gap state see a much higher bath temperature to T_c ratio, which results in a larger than expected population of thermally excited quasiparticles. To detect a double gap in a superconducting material, one can measure the dependence on temperature of a superconducting resonator's resonant frequency. If the data is a good fit for one BCS gap at high temperatures and a good fit for a different BCS gap at low temperatures, this is evidence for a double gap or multi-gap material. This behavior is easiest to see and understand by looking at the dependence on $1/T$ of $log(1-(f(T)/f(0))^2)$, which should be linear with a slope $m = -\Delta/k$ in the low-temperature limit. Figure 4 shows the 0 mG B_{Earth} data from the test chip displayed in this manner. The dashed line shows the relatively poor best fit for a simple single-gap model. The solid line shows a substantially better fit to the data by allowing 11.1% of the $1/L_k$ to come from a low-gap state with $\Delta = 0.4 \times \Delta_{BCS}$ (i.e. a superconducting energy gap which is only 40% of the gap energy expected from a simple BCS prediction) and the remainder of $1/L_k$ coming from a typical gap state with $\Delta = 0.75 \times \Delta_{BCS}$. Figure 5 shows an alternative view of the same data set, now with inverse internal quality factor and inverse bath temperature for two resonators with the lowest and highest internal Qs. The solid line shows the expected Q_is for a simple two-gap model with parameters as described in figure 4. However, figure 3 shows that at low temperature, Q_i saturates as a result of an unknown temperature-independent dissipation. The dashed lines show the two-gap prediction for Q_i with two different constant values added in to account for the unknown additional dissipation. When the additional constant dissipation term is included, the two-gap model is a good fit for the data.

An alternative explanation for this data is the Klapwijk model for gap broadening in disordered superconductors.[9] Distinguishing the two-gap model from the gap-broadening model in our samples will require additional

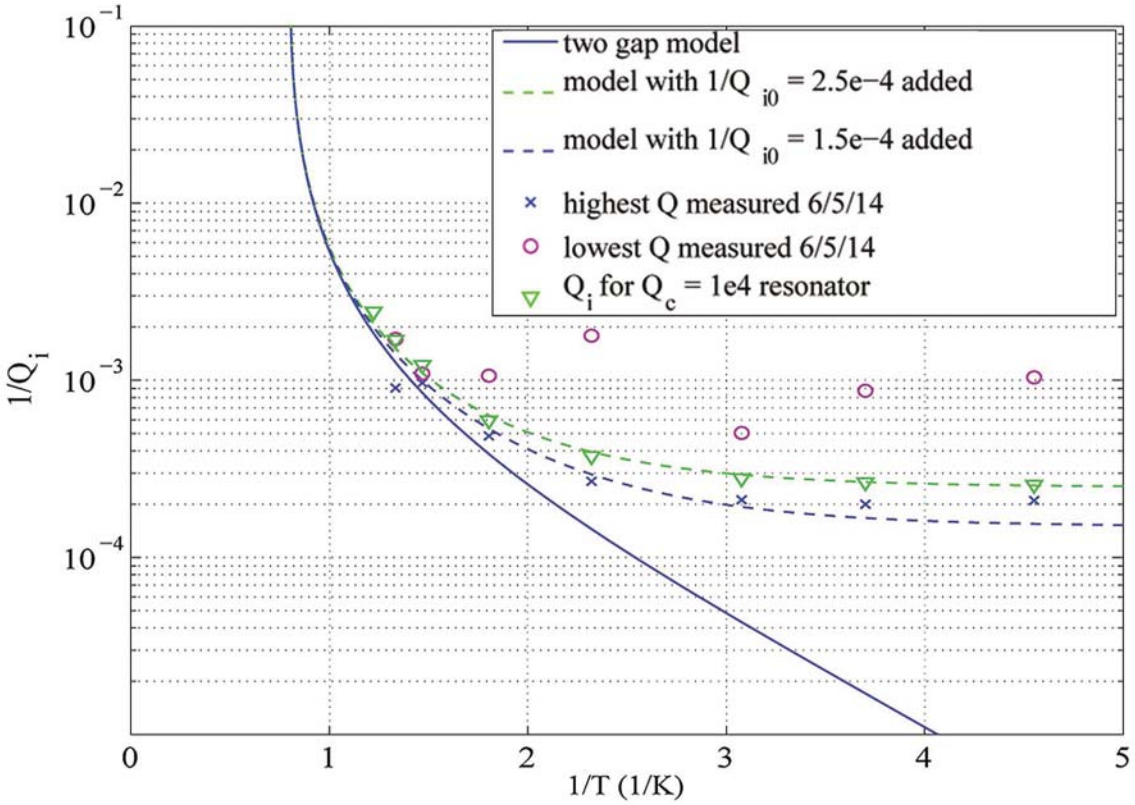

Figure 5. Two-gap fit to the data, with and without an additional temperature-independent dissipation term. The purple circles are the data from the resonator with the lowest internal Q. The blue x marks are the data from the resonator with the highest internal Q. The green triangles are the data from the resonator with the best-matched coupling Q, $Q_c = 1 \times 10^4$. The solid blue line is the expectation for a simple two-gap model. The dashed blue and green lines are expectations for two gap models with, respectively, 1.5×10^{-4} and 2.5×10^{-4} added to $1/Q_i$ to account for the observed temperature-independent dissipation.

data.

5. CONCLUSIONS

We are developing a prototype KID array for the QUBIC telescope, optimized for 3 mm observations at 100 mK. We observe significantly lower than expected Qs in our resonators. These low total quality factors are attributable to lower than expected internal quality factors, however we have not yet definitively determined the source of the unanticipated internal dissipation. We have determined that orientation of the detector chip relative to Earth's magnetic field is an important consideration, however this is insufficient by itself to explain the discrepancy between observation and theory.

There is some concern that, despite the magnetically shielded housing for the 3 T ADR magnet, there may be enough field leakage that the device quality factor may be affected. The worst-case leaked field from the ADR perpendicular to the plane of the chip is of the same order as Earth's magnetic field, however we believe the actual leaked field is likely to be much smaller than Earth's field. Future work will include measuring the actual ADR field near the chip during a cooldown and adding additional magnetic shielding either to the ADR housing or to the chip housing based on simulations currently underway.

We have also found some evidence for double superconducting gap behavior in the Mo resonators. The low-gap population of electrons may be sufficient to relieve the tension between the expected and observed internal quality factors, however additional data will be required to definitively confirm or rule out this explanation.

ACKNOWLEDGMENTS

This work was supported by a NASA Office of the Chief Technologist's Space Technology Research Fellowship. The authors also acknowledge Kevin Denis of NASA Goddard Space Flight Center for his valuable assistance with device fabrication.

REFERENCES

[1] Day, P. K., LeDuc, H. G., Mazin, B. A., Vayonakis, A., and Zmuidzinas, J., "A broadband superconducting detector suitable for use in large arrays," *Nature* **425**, 817 (Oct 2003).

[2] Battistelli, E., Baú, A., Bennett, D., Bergé, L., Bernard, J.-P., de Bernardis, P., Bordier, G., Bounab, A., Bréelle, É., Bunn, E. F., Calvo, M., Charlassier, R., Collin, S., Coppolecchia, A., Cruciani, A., Curran, G., de Petris, M., Dumoulin, L., Gault, A., Gervasi, M., Ghribi, A., Giard, M., Giordano, C., Giraud-Héraud, Y., Gradziel, M., Guglielmi, L., Hamilton, J.-C., Haynes, V., Kaplan, J., Korotkov, A., Landé, J., Maffei, B., Maiello, M., Malu, S., Marnieros, S., Martino, J., Masi, S., Murphy, A., Nati, F., O'Sullivan, C., Pajot, F., Passerini, A., Peterzen, S., Piacentini, F., Piat, M., Piccirillo, L., Pisano, G., Polenta, G., Prêle, D., Romano, D., Rosset, C., Salatino, M., Schillaci, A., Sironi, G., Sordini, R., Spinelli, S., Tartari, A., Timbie, P., Tucker, G., Vibert, L., Voisin, F., Watson, R. A., Zannoni, M., and QUBIC Collaboration, "Qubic: The qu bolometric interferometer for cosmology," *Astroparticle Physics* **34**, 705 (2011).

[3] Zmuidzinas, J., "Superconducting microresonators: Physics and applications," *Annual Review of Condensed Matter Physics* **3**(1), 169–214 (2012).

[4] Iavarone, M., Karapetrov, G., Koshelev, A., Kwok, W. K., Hinks, D., Crabtree, G. W., Kang, W. N., Choi, E.-M., Kim, H. J., and Lee, S.-I., "Mgb 2 : directional tunnelling and two-band superconductivity," *Superconductor Science and Technology* **16**(2), 156 (2003).

[5] Kim, M.-S., Skinta, J. A., Lemberger, T. R., Kang, W. N., Kim, H.-J., Choi, E.-M., and Lee, S.-I., "Reflection of a two-gap nature in penetration-depth measurements of mgb_2 film," *Phys. Rev. B* **66**, 064511 (Aug 2002).

[6] Choi, H. J., Roundy, D., Sun, H., Cohen, M. L., and Louie, S. G., "Superconducting energy gaps, low temperature specific heat, and quasiparticle spectra of MgB2," *eprint arXiv:cond-mat/0111183* (Nov. 2001).

[7] Pickett, W., "Superconductivity: Mind the double gap," *Nature* **418**(6899), 733–734 (2002).

[8] Binnig, G., Baratoff, A., Hoenig, H., and Bednorz, J., "Two-band superconductivity in nb-doped srti o 3," *Physical Review Letters* **45**(16), 1352 (1980).

[9] Coumou, P. C. J. J., Driessen, E. F. C., Bueno, J., Chapelier, C., and Klapwijk, T. M., "Electrodynamic response and local tunneling spectroscopy of strongly disordered superconducting tin films," *Phys. Rev. B* **88**, 180505 (Nov 2013).